Fluorescein isothiocyanate stability in different solvents

Dytrtova, Jana Jaklova

2021-11

Dytrtova , J J , Moslova , K , Jakl , M , Siren , H & Riekkola , M-L 2021 , ' Fluorescein isothiocyanate stability in different solvents ' , Monatshefte für Chemie , vol. 152 , no. 11 , pp. 1299-1306 . https://doi.org/10.1007/s00706-021-02852-1

http://hdl.handle.net/10138/349771
https://doi.org/10.1007/s00706-021-02852-1

acceptedVersion

Dynamic simulation of nutrient distribution in lakes during ice cover growth and ablation

Abstract:

Nutrient transport in seasonally ice-covered lakes is an important driver of spring algal blooms in eutrophic waters because phase changes during the ice growth process redistribute the nutrients. In this study, nutrient transport under static conditions was simulated using two ice thickness models in combination with an indoor freezing experiment under different segregation coefficient conditions for nutrients. A real-time prediction model for nutrient and pollutant concentrations in ice-covered lakes was established to explore the impact of the ice-on period in eutrophic shallow lakes. The results showed that the empirical degree-day model and the high-resolution thermodynamic snow and sea-ice model (HIGHTSI) could both be used to simulate lake ice thickness. The empirical degree-day model performed better at predicting the maximum ice thickness (measured thickness 0.22–0.55 m; simulated thickness 0.48 m), while the HIGHTSI model was more accurate when estimating the mean thickness (5–6 % error). When simulating ice growth, the HIGHTSI model considered more meteorological factors impacting ice cover ablation; hence, it performed better during the ablation stage relative to the empirical degree-day model. Two non-dynamic nutrient transport models were developed by combining the segregation coefficient model and the ice thickness prediction model. The HIGHTSI nutrient transport model can be used to predict real-time changes in nutrient concentrations under ice cover, and the degree-day model can be used to predict changes in the lake water ecosystem.

Key words: seasonal ice-cover, eutrophic lakes, high-resolution thermodynamic snow and sea-ice model, empirical degree-day model, nutrient migration

1. Introduction

The impact of climate change on high-latitude and polar regions has strengthened concerns related to the formation and melting of ice cover in lakes, the effects of ice-water energy exchange, and the environment of frozen lakes and polar ecosystems (Kirillin et al. 2012, Prowse 2001, Zhang et al. 2020, Zhang et al. 2013). Compared to tropical or subtropical regions, inland waters (rivers, lakes, reservoirs) at mid and high latitudes in the northern hemisphere contain higher concentrations of dissolved organic matter and nutrients (Song et al. 2019, Yang et al. 2019). There are many unanswered questions regarding climate change-driven eutrophication of seasonally ice-covered lakes; hence, further research is required (Ho et al. 2019).

Studies have found that the under-ice electrical conductivity in glacial lakes changes during freeze-thaw cycles due to the high concentration of nutrients released by the ice sheet (Boetius et al. 2015, Fountain et al. 2008). Simulation experiments have demonstrated that the concentration of total manganese (TMn) in under-ice water is up to 0.27 times higher than before freezing (Zhang et al. 2019). In shallow lakes, winter electric conductivity was found to be 1.7–2.7 times the summer value, and the elevated salt content in lake water was caused by the exclusion of more than 97% of salt from the lake ice-cover (Pieters and Lawrence 2009). Furthermore, Leppäranta et al. (2003) and Zhang et al. (2012) found that during the ice growth period, approximately 80% of the total dissolved solids were excluded from the ice and remained in the underlying water layer. Studies on the nutrient cycles of seasonally ice-covered shallow lakes (such as Lake Washington) found that the maximum concentrations of salts (P and N) occurred during winter and that P and N accumulated in under-ice water were the primary nutrients available to phytoplankton during summer (Bullerjahn et al. 2019, Edmondson 1970, Yang et al. 2019). Seasonal ice cover in shallow lakes reduces the volume of liquid water in the lake and significantly increases the under-ice nutrient concentration, increasing the risk of algal blooms (Agbeti and Smol 1995, Pennak 1968, Powers et al. 2017).

Controlling the concentration of nutrients in lake ecosystems is an important strategy for environmental risk management (Feng et al. 2018). The majority of previous studies on lake eutrophication have been conducted during ice-off periods; however, lake pollution differs between ice-on and ice-off periods (Cloete et al. 2019, Wu and Qian 2003). Therefore, more research is required to determine how nutrient-salt concentrations in lake water during ice-on periods affect geochemical processes; for example, dissolved oxygen concentration, algal growth, and organic matter degradation (Huang et al. 2019, Kirillin et al. 2012, Song et al. 2019).

During the ice-on period, lake temperature and solar radiation are low. The flow of matter and energy in the lake ecosystem tends to be slow. Furthermore, during the formation of ice cover on the lake, pure water is consolidated into a layer of ice, while nutrients and impurities are largely excluded into the underlying water, causing a rapid increase in nutrient concentrations under the ice (Song et al. 2019, Yang et al. 2016b, Zhang et al. 2012) which impacts the ice-covered lake ecosystem. However, the observation and simulation methods for this phenomenon are not yet well established (Bai et al. 2016, Yang et al. 2017). Under near-anoxic conditions and relatively low biological activity during winter, organic matter at the lake bottom is decomposed through physical and biochemical processes, including sedimentation, adsorption, and biodegradation (Agbeti and Smol 1995, Bostrom et al. 1988, Palmer et al. 2019, Song et al. 2019). During the ice-on period, sediments act as a sink by storing accumulated nutrients. During the ice-off period, sediments act as a source, releasing nutrients into the overlying water as the ice cover melts and the concentration of solutes in the water decreases. Studies have indicated that when exogenous pollution is controlled, the continuous release of nutrients into the overlying water body by sediments is an endogenous cause of lake eutrophication (Feng et al. 2016, Zhao et al. 2014).

The dynamic nature of nutrient concentrations in the ice-covered water environment becomes increasingly difficult to observe as the ice cover grows. Ice layers can only be sampled after reaching a certain thickness, so it is easy to miss relevant data during the initial freeze-up and the final break-up stages. Furthermore, long-term observations of the low-temperature water environment during the ice-on period are challenging for the measuring equipment (Lu et al. 2018, Yu et al. 2013, Yang et al. 2020). For example, portable nutrient analyzers require in-situ sampling and have many limitations when used in environments below the freezing point temperature, resulting in unreliable observations or instrument damage.

This paper proposes a new model for predicting changes in the nutrient concentration of ice-covered water environments. Our proposed model simulates nutrient transport with ice cover growth in shallow lakes by representing the dynamic relationship between the ice growth and the consequent change in the quality of the underlying water using the principles of water balance and water quality balance. The concept of simulating the under-ice water environment based on hydrometeorological data can overcome the challenges of unreliable monitoring equipment and insufficient data during the freeze-up and break-up periods. Simulations also can provide valuable data regarding the dynamic nature of under-ice nutrient concentrations caused by the growth of the ice cover in shallow lakes.

2. Methods and Materials

2.1 Research area and sample collection

Ulansuhai Lake is a typical seasonally ice-covered lake in northern China. Its ice-on period lasts 4–5 months (November–April) with a maximum ice thickness of 0.7 m (Yang et al. 2016b, Zhang et al. 2012, Yang et al. 2020). The monitoring points of Ulansuhai Lake are shown in Fig. 1. Ice cores and water samples were collected during the winter months of 2010–2014 for ice thickness, ice crystal structure and density, and ice meltwater and under-ice water quality (Yang et al. 2016a). The water quality data included total nitrogen (TN), and total phosphorus (TP). Three samples were taken at each site for these ice and water properties . The TN content was determined using the potassium persulfate digestion–UV spectrometry method, and the TP content was measured using the molybdenum-antimony anti-spectrophotometric method (EPA of China 1989). Ice thickness was simulated using atmospheric temperature data for the ice-on period from October 10, 2006 to April 30, 2014, collected by the meteorological station no. 53433 (41.0167 ºN, 109.1333 ºE, and located 9 km to the east of the lake.) and obtained from China's Integrated Meteorological Information Service System.

2.2 Empirical degree-day model

Due to sampling limitations posed by the harsh environment, the thickness of the ice cover was calculated using the degree-day method for the thermal growth (Shen and Chiang 1984, Shen and Yapa 2011, Zubov 1963). The thickess of ice is proportional the the square root of the freezing-degree-days θ, with value of the empirical proportionality coefficient A_0 under different ice cover conditions obtained from another publication (Table 1, Michel and Ramseier 1971). Assuming that A_0=2.7 cm $C^{-½}$ $day^{-½}$, the empirical equation for ice thickness, H, (SI.2 for the derivation) is:

$$H=0.027\ \theta^{1/2} \tag{1}$$

2.3 One-dimensional high–resolution thermodynamic snow/ice model

The one-dimensional high-resolution thermodynamic snow/ice model HIGHTSI has been used to obtain accurate simulations of the growth and melting of ice cover in the Bohai, Baltic, and Arctic Seas (Cheng et al. 2006, Karvonen et al. 2017, Merkouriadi et al. 2017, Yao et al. 2016). With parameter optimization and adjustment to account for the differences between sea and lake conditions (Table 3, SI Fig.1 and Table 2), the HIGHTSI model has also demonstrated good results in simulating the growth of ice and snow in freshwater lakes and reservoirs, including the Vanajavesi and Kilpisjárvi Lakes in Finland (Yu et al. 2013).

During the ice-on period, the consolidation of the relatively pure lake water into ice cover is the main physical driver for the water quality evoltution in shallow lakes. Naturally, other accompanying ecological factors also affect the water quality, but, however, this study focuses on the effect of ice growth and ablation. We assume that the nutrient concentration of under-ice water in winter is only affected by the amount of water consolidated into ice and the release of nutrients in the freezing process. In other words, the ice thickness determines the amount of water consolidated into the ice cover, which in turn determines the nutrient concentration of the underlying water. Based on the two different models for ice thickness, coupled with the one-dimensional equations of water balance and water quality under static ice growth conditions, a model of the nutrient transport process in the under-ice water environment during the ice-on period was developed. The model can predict the evolution of the nutrient concentration of under-ice water during ice cover growth and ablation.

2.4 Nutrient transport model under static ice conditions during the ice-on period

A simulation experiment was carried out to obtain the segregation coefficient for nutrients in ice growth. The experiment was a controlled process of ice sheet growing downward from the surface close to natural conditions as much as possible (Detail information is shown in SI3. Table 1 shows the segregation coefficients of nutrients in ice growth, $\kappa = \frac{\bar{C}_i}{C_w}$. It is evident that as the initial concentration decreased, the ice-water distribution coefficient increased. The segregation coefficients of TP and TN were 0.33–0.12 and 0.50–0.30, respectively. In practical applications, an appropriate coefficient can be selected based on the initial concentration of lake water nutrients before the formation of ice cover to estimate the nutrient content of water under the ice. Table 2 shows the segregation coefficients of nutrients, ice, and the underlying water at different temperatures. As the temperature decreases, the segragation coefficients increase markedly, showing that the cooling rate in early winter has a considerable impact on the concentration of nutrients in the ice cover.

The basic equations for one-dimensional water balance and water quality evolution under static ice conditions were analyzed for a water column (Fig. 2, SI.2, Table 1).

1) The basic equation of water balance can be expressed as:

$$\frac{dV}{dt} = -\frac{\rho_i}{\rho_w} h_i \cdot A \tag{2}$$

where $\frac{dV}{dt}$ is the rate of change of the liquid water volume, h_i is the freezing rate of the ice cover, ρ_i is the density of ice (910 kg/m^3), ρ_w is the density of water (1000 kg/m^3), and A is the base area of the unit column (1 m^3). It is evident from Eq. 2 that the mass of ice in the unit column is equal to the mass of reduced water, and the mass of water in the entire column remains unchanged.

2) The basic equation of water quality evolution can be expressed as :

$$\frac{dVC}{dt} = A \cdot \frac{\rho_i}{\rho_w} C_w^k \cdot H_i^k - A \cdot \frac{\rho_i}{\rho_w} C_i^k \cdot H_i^k \tag{3}$$

where C_w^k is the solute concentration before dt, C_i^k is the solute concentration of the ice layer formed, and H_i is the increase of ice thickness. In the HIGHTSI model, $H_i = h_i$, and in the empirical degree-day model, $H_i = 0.027\theta(t)^{\frac{1}{2}}$. It is evident from Eq. 3 that the amount of pollutants discharged from the ice cover is equal to the increase of pollutants in the water column underlying the ice in a unit of time.

With the segregation coefficient $\kappa = C_i^k / C_w^k$, the equation can be simplified to:

$$\frac{dVC}{dt} = (1-k) A \cdot \frac{\rho_i}{\rho_w} C_w^k \cdot H_i^k \tag{4}$$

Under the initial ice-free conditions: $M_0 = A \cdot C_w^0 \cdot H_0$; where M_0 is the initial concentration of the water column per unit area before freezing, C_w^0 is the initial concentration of the target substance *k,* and H_0 is a constant representing the mean water depth.

The model boundary conditions can be expressed as:

$$H_w = H_0 - H_i;\ \text{when}\ H_i = 0,\ C_i^k = 0. \tag{5}$$

3. Results and analyses

3.1 Analyses of empirical degree-day model results

Ice cover thickness was simulated using the empirical degree-day model (Eq. 1) and compared with observations. Ice cover began to form on the lake surface on November 10, 2013, reaching a maximum thickness on February 22, 2014 (Fig. 3). There were 104 consecutive days with temperatures below 0 ºC, and the cumulative negative temperature was -799.3 ºC·d. The maximum ice thickness of 0.55 m was measured at the sampling point J11 on January 15, 2014, and the minimum ice thickness of 0.22 m was observed at P11. The mean ice thickness of the entire lake was 0.48 m. In comparison, the maximum ice thickness calculated using the degree-day simulation method for January 15, 2014, was 0.62 m, which was relatively close to the observed value.

The empirical degree-day model was used to simulate the ice cover thickness in 2007–2014 based on temperature data from October 10, 2007 to April 30, 2014. The calculation began when the temperature is below 0 ºC for three consecutive days, and the maximum ice thickness was calculated when the temperature was above 0 ºC for three consecutive days (Table 4). Fig. 4 shows the comparison between the simulated and the measured values of ice thickness from 2007–2014. Due to the varying ice conditions and the consequent safety considerations, sampling times and quantities differed from year to year (in Fig. 4, the number on top of the column represents the number of sampling points). The mean ice thickness of the lake was obtained by taking the mean ice thickness at each point. The maximum ice thickness predicted for 2007–2014 using the degree-day method was close to the calculated value, indicating that the model can be used to predict the maximum ice thickness in Ulansuhai Lake during the ice-on period.

3.2 Analysis of HIGHTSI model results

Fig. 5 shows the growth of ice cover simulated using the HIGHTSI model. The mean simulated thickness was within 15% of the measured value. In 2010 and 2011, the calculated values of the mean ice thickness during the ice-on period were lower than the measured values (an error rate of 5%); conversely, the calculated values were slightly higher than the measured values (an error rate of 3–6%) for the remainder of the period. Model errors can be attributed in part to the accuracy of the meteorological data. In this study, data from a single observation station was used. Precipitation was assumed to be evenly distributed on the lake surface, and the depth of water under the ice was assumed to be uniform, i.e., the whole lake was treated as a single entity, and the results are considered representing the average. Furthermore, precipitation was abundant during the winters of 2010 and 2011, so the snow layer simulated by the model was relatively thick, impacting the heat flux from the atmosphere to the ice (Zhao et al. 2019). Because the snow cover on the ice surface was not uniform and the observed ice thickness also varied, the uniform values simulated by the HIGHTSI model differed from the measurements. Finally, Ulansuhai Lake is often windy during winter, and therefore snowfall can be cleared from the lake by the wind. A bare ice cover has a high transmittance so that in a sunny winter day, the water under the ice still receives a large amount of solar radiation. HIGHTSI model only considers the impact of snowmelt for ablation and wind effects are ignored. For example, a short-term warming in mid-January 2014 should have slowed down the simulated ice growth, but, however, the model did not account for the removal of a thin snow layer by the wind and maintained rapid growth; hence, the simulation did not reflect the actual ice conditions. These results can also be related to the shallow water depth and faster rate of heat loss of Ulansuhai Lake (Huang et al. 2019, Song et al. 2019, Yang et al. 2016b, Yang et al. 2019).

The HIGHTSI simulation of Vanajavesi Lake (Yang et al. 2012) showed a lower snow thickness compared to observations. A similar underestimation of snow cover was found in the simulation of Lake Pääjärvi (Kärkäs 2000). Based on these findings, it is reasonable to conclude that the error in the ice thickness estimation in the HIGHTSI simulation of

Ulansuhai Lake is related to the treatment of snow cover in the model. Considering the overall performance of the HIGHTSI model, with the average difference between the simulated and the measured values in a four-year simulation ranging from 5–6%, we conclude that this model can be used to accurately predict the ice growth in Ulansuhai Lake.

3.3 Analysis of lake characteristics during the ice season

Based on the analysis of temperature data from 2007–2013 and the monitoring data of TN and TP under the ice cover (Fig. 6), it is apparent that the date when the air temperature begins to rise shifts earlier year by year, indicating that ice cover thaw might also occur earlier (Table 3). For this reason, the annual ice cover thickness calculated by the degree-day model also showed a decreasing trend. During the ice-on seasons in 2008–2014, the trends of TN and TP concentrations under the ice cover were generally consistent with those of ice thickness (Fig. 6). It is worth noting that the ice-on period was relatively long in 2007–2008 and 2011–2012 (over 110 days), and the ice cover was predicted to be thicker in these two seasons. The predicted ice thickness was 0.792 m in 2007–2008 and 0.755 m in 2011–2012, accounting for 56.6% and 53.9% of the mean water depth, respectively. The mean TN content under the ice cover was 6.95 mg/L in 2007–2008 and 8.189 mg/L in 2011–2012, which was 1.9 and 3.1 times the TN content in the lake before freeze-up occurred in October 2007 and 2011, respectively; the TP content was 0.28 mg/L in 2007–2008 and 0.30 mg/L in 2011–2012, which was, respectively, 1.5 and 1.7 times the TP content in the lake before freeze-up. In these two years, the measured nutrient concentration in the lake was higher during the ice-on period. The evolution of the nutrients in the water should be directly related to the ice thickness evolution. On one hand, nutrients were rejected to water under the ice during the ice growth, and on the other hand, mostly pure water was consolidated into ice. The changes were also clearly reflected in the predicted ice thickness values.

In 2014, there was a marked difference between the measured change in the nutrient concentration and the simulated change in ice thickness during the ice-on period. This can be attributed to the city of Bayannur greatly increasing the water supply to Ulansuhai Lake since 2012 that enhanced the metabolic capacity and self-purification capabilities of the lake, and resulting in a significant improvement in water quality (Hao et al. 2014, Wang et al. 2018).

3.4 Simulation results of dynamic nutrient-change in ice-covered water during the ice-on period

During the ice-on period from October 2011 to May 2012, the initial simulation conditions included a mean lake water depth of 1.26 m, and mean concentrations of TN and TP in lake water before ice formation of 2.634 and 0.306 mg/L, respectively. When the ice thickness reached 30.5% of the lake water depth, the mean concentrations of TN and TP under the ice were 3.589 and 0.452 mg/L, respectively. These two values served as the validation points. The simulation results are shown in Figs. 7 and 8.

Fig. 7(a) shows the evolution of the lake water TN concentration based on the HIGHTSI simulation of the ice cover. When the segregation coefficient was 0.5 (0.3), the relative error between the calculated and measured values was 7% (6%). Fig. 7(b) shows the evolution in the lake water TN content based on the ice-cover simulation using the empirical degree-day model. When the segregation coefficient was 0.5 (0.3), the relative error between the calculated and measured values was 7% (2%).

Fig. 8(a) shows the evolution of the lake water TP concentration based on the ice cover simulation using the HIGHTSI model. When the segregation coefficient was 0.12 (0.33), the relative error between the calculated and measured values was relatively high, 9% (11%). Fig. 8(b) shows the evolution in the lake water TP concentration based on the ice-cover simulation using the empirical degree-day model. When the segregation coefficient was 0.12 (0.33), the relative error between the calculated and measured values was –6% (4%).

Compared with the observations, the simulation errors using the HIGHTSI model and the empirical degree-day model ranged within 7–11%, indicating that both models are suitable for simulating the evolution of TN and TP concentrations during the growth and ablation of ice cover.

4 Discussion

4.1 Comparative analysis of dynamic nutrient-concentration simulations

Previous studies have shown that as ice cover grows and melts, the solute concentration under the ice cover changes markedly (Zhang et al. 2013, Zhang et al. 2012, Zhang et al. 2019). Studies have also found that both shallow and deep lakes (depth ≥ 6 m) show a close relationship between the water conditions under the ice cover and the peak values of nutrients in spring and summer (Agbeti and Smol 1995, Shen et al. 2020, Sondergaard et al. 2017).

In this study, two types of ice thickness models were used to simulate the evolution of nutrient concentrations in lake water using different segregation coefficients during the ice-on period. Considering the difference of the level of the two models, the relative error of the advanced HIGHTSI model for lake water nutrients with different segregation coefficients was slightly higher; however, its mean ice thickness was more accurate (relative error of 5–6%), indicating that the model is suitable for estimating the thickness of the seasonal ice cover in shallow lakes. We found that the empirical degree-day model, which uses air temperature data, is suitable for predicting the maximum ice thickness and can be used for practical applications. Both models provided a good estimation of ice cover growth; however, the HIGHTSI model considered more meteorological factors, and its simulation of ice cover changes at the end of the ice-on period was closer to actual conditions. Conversely, the empirical degree-day model only considered air temperature changes, and the simulation deviated from the actual conditions, making the model unsuitable during the ablation period.

4.2 Accuracy analysis for nutrient distribution and ice thickness

The air temperature was the only forcing factor to simulate the ice thickness in the empirical degree-day method, while the HIGHTSI, considering more advanced heat flux calculation, needed nine factors to forecast the ice thickness. When the data was sufficient and detailed, ice thickness simulation was more accurate using HIGHTSI, and the empirical degree-day method would be more appropriate for insufficient forcing data. In this study, the evolution of the nutrient concentrations in the water were directly related to the ice thickness evolution.

The ice thickness simulation errors were mainly due to two factors. Firstly, during ice melting, the ice hardness is decreasing and ice becomes soft and porous, broken easily by the external force or even by own weight. This process is not fully provided by HIGHTSI, which is based on the thermodynamic processes at the top and bottom surcaces without the breaking process. Secondly, HIGHTSI has a high demand for data, which requires nine forcing factors to forecast the ice thickness. Most of the monitoring data are 8 hours apart, and the input data is required at 1-hour interval. Therefore, data deficits often bring errors, but, however, HIGHTSI has been proved good in many application cases (Bear Lake， Lake Vanajavesi， Lake Orajärvi, and so on), and its accuracy and sensitivity have advantages in the lake ice prediction (Tido et al. 2012, Yang et al. 2012, Cheng et al. 2020).

Considering the accuracy of the models in estimating the nutrient load in the ice-covered water environment, we found that the accuracy of the preliminary simulations reached 85%. Thus, this method can provide an important theoretical basis for environmental protection and health inspection of ice-covered lakes.

4.3 Simulation and early warming of eutrophication

Dissolved oxygen cannot be replenished under heavy ice cover, and the existing oxygen storage is continuously consumed during the ice-on period (Bai et al. 2016, Feng et al. 2018, Yan et al. 2019, Yang et al. 2017). Studies have found that primary production and photosynthetic efficiency of ice-covered lakes are impacted by solar radiation intensity and water temperature (e.g., Song et al. 2019). In high latitudes and in the presence of snow on ice, photosynthetic activity is low which makes it impossible for dissolved oxygen to be replenished. Therefore, the reduction of solar radiation by ice cover (low light transmittance, such as snow and ice) can reduce or even stop photosynthetic activity in lake water (Zhao et al. 2019), leading to oxygen depletion and fish death (Golosov et al. 2007, Kirillin et al. 2012). Moreover, nutrient consumption is slower in winter compared to other seasons, resulting in the accumulation of nutrients and organic matter (Golosov et al. 2007, Ho et al. 2019, Song et al. 2019, Zhang et al. 2020). Studies of Donghu and Chaohu Lakes showed that the chlorophyll-a concentration and nutrient consumption in winter were significantly lower compared to other seasons (Deng et al. 2007, Lei et al. 2005).

In recent years, there have been two large-scale algal blooms in Ulansuhai Lake. The first one occurred in May 2008, when approximately 54 km^2 of yellow algae appeared on the central lake surface and remained for nearly 5 months (Wei 2010). This event led to the implementation of remedial measures. The second event occurred on May 28–31, 2012, impacting the second largest fishery in Inner Mongolia (Guo et al. 2015, Yuanyuan et al. 2018). Our results show that the ice-on periods in 2007–2008 and 2011–2012 were relatively long (>110 d), the ice was relatively thick, and the nutrient accumulation load was high, which may have triggered the subsequent spring algal bloom events. These events highlight the importance of simulating the growth and ablation of lake ice and ice-water nutrient fluxes during ice season. Furthermore, our results indicate that the empirical degree-day and the HIGHTSI models have the potential to be used as an early warning system for algal blooms following the ablation of lake ice cover in cold and dry regions.

5. Conclusions

A model was established to simulate real-time nutrient concentrations in lake water during the growth and ablation of ice cover. Static ice models were used to simulate nutrient loads in ice-covered lake water by combining different segregation coefficient data and ice thickness predictions under different control conditions. The preliminary prediction of the nutrient model can be used to forecast changes in the lake water ecosystem in the next step. This study provides a theoretical basis for ongoing pollution management of ice-covered lakes. The main conclusions are as follows:

1) The empirical degree-day model can be used to predict the maximum thickness of lake ice based on air temperature data. However, the HIGHTSI model can provide more accurate simulations of lake ice cover during the ice-on season, because it incorporates temperature, wind speed, relative humidity, cloud cover, and precipitation data.

2) During the ice growth period, both the empirical degree-day model and the HIGHTSI model accurately predicted ice thickness; however, during the ablation period, the HIGHTSI simulation was more accurate.

3) Ice thickness simulations can be used to accurately predict nutrient concentrations in ice-covered lake water, providing an important indicator and early warning system for changes in the lake water environment after ice-on.

Acknowledgments

This research was jointly supported by the National Natural Science Foundation of China (41907338, YFC0409205, 41703115, and 41573124), Postdoctoral Science Foundation of China (2019M660753), and Youth Top Talent Support Program of Beihang University (YWF-20-BJ-J-907). The authors would like to thank Prof. Changyou Li for study design and data collecting from Inner Mongolia Agricultural University, Hohhot, China.

References

Agbeti, M.D. and Smol, J.P. (1995) Winter limnology: a comparison of physical, chemical and biological characteristics in two temperate lakes during ice cover. Hydrobiologia. 304(3), 221-234.DOI: 10.1007/BF02329316

Bai, Q., Li, R., Li, Z., Lepparanta, M., Arvola, L. and Li, M. (2016) Time-series analyses of water temperature and dissolved oxygen concentration in Lake Valkea-Kotinen (Finland) during ice season. Ecological Informatics. 36(11), 181-189. DOI:10.1016/j.ecoinf.2015.06.009

Boetius, A., Anesio, A.M., Deming, J.W., Mikucki, J.A. and Rapp, J.Z. (2015) Microbial ecology of the cryosphere: sea ice and glacial habitats. Nature Reviews Microbiology. 13(11), DOI:677-690.10.1038/nrmicro3522

Bostrom, B., Andersen, J.M., Fleischer, S. and Jansson, M. (1988) Exchange of phosphorus across the sediment-water interface. Hydrobiologia. 170(1), 229-244. DOI:10.1007/978-94-009-3109-1_14

Bullerjahn, G.S., Mckay, R.M.L., Bernat, G., Prasil, O., Voros, L., Palffy, K., Tugyi, N. and Somogyi, B. (2019) Community dynamics and function of algae and bacteria during winter in central European great lakes. Journal of Great Lakes Research. In press, corrected proof available online 19 July 2019.DOI: 10.1016/j.jglr.2019.07.002

Cheng, B., Vihma, T., Pirazzini, R. and Granskog, M.A. (2006) Modelling of superimposed ice formation during the spring snowmelt period in the Baltic Sea. Annals of Glaciology. 44, 139-146. DOI:10.3189/172756406781811277

Cheng, Y., Cheng, B., Zheng, F., Vihma, T., Kontu, A., Yang, Q. and Liao Z. (2020). Air/snow, snow/ice and ice/water interfaces detection from high-resolution vertical temperature profiles measured by ice mass-balance buoys on an Arctic lake. Annals of Glaciology 1–11. https://doi.org/10.1017/ aog.2020.51

Cloete, R., Loock, J.C., Mtshali, T.N., Fietz, S. and Roychoudhury, A.N. (2019) Winter and summer distributions of Copper, Zinc and Nickel along the International GEOTRACES Section GIPY05: Insights into deep winter mixing. Chemical Geology. 511, 342-357.DOI: 10.1016/j.chemgeo.2018.10.023

Deng, D., Xie, P., Zhou, Q., Yang, H. and Guo, L. (2007) Studies on Temporal and Spatial Variations of Phytoplankton in Lake Chaohu. Journal of Integrative Plant Biology. 49(4), 409-418. DOI:10.1111/j.1744-7909.2007.00390.x

Edmondson and T., W. (1970) Phosphorus, Nitrogen, and Algae in Lake Washington after Diversion of Sewage. Science. 169(3946), 690-691. DOI: 10.1126/science.169.3946.690

EPA of China. (1989) The method of monitoring and analyzing water and wastewater. Beijing, China: Environmental Science Press House.

Feng, W., Wu, F., He, Z., Song, F., Zhu, Y., Giesy, J.P., Wang, Y., Qin, N., Zhang, C., Chen, H. and Sun, F. (2018) Simulated bioavailability of phosphorus from aquatic macrophytes and phytoplankton by aqueous suspension and incubation with alkaline phosphatase. Science of The Total Environment. 616-617, 1431-1439. DOI:10.1016/j.scitotenv.2017.10.172

Feng, W., Zhu, Y., Wu, F., He, Z., Zhang, C. and Giesy, J.P. (2016) Forms and Lability of Phosphorus in Algae and Aquatic Macrophytes Characterized by Solution 31P NMR Coupled with Enzymatic Hydrolysis. Scientific Reports. 6(1), 37164-37164. DOI: 10.1038/srep37164

Fountain, A.G., Nylen, T.H., Tranter, M. and Bagshaw, E. (2008) Temporal variations in physical and chemical features of cryoconite holes on Canada Glacier, McMurdo Dry Valleys, Antarctica. Journal of Geophysical Research. 113, 1-11. DOI: 10.1029/2007JG000430

Golosov, S., Maher, O.A., Schipunova, E., Terzhevik, A., Zdorovennova, G. and Kirillin, G. (2007) Physical background of the development of oxygen depletion in ice-covered lakes. Oecologia. 151(2), 331-340. DOI:10.1007/s00442-006-0543-8

Guo, J., Wei, W., Yi-Lei, Y.U., Song, X.J., Zhang, M.Y. and Sheng-Nan, L.I. (2015) Research progress on the eutrophication of Ulansuhai wetland. Chinese Journal of Ecology.Chinese.

Hao, Y., Yu, R.H., Zhang, Y.J. and Yang, H. (2014) The Relationship of Chlorophyll-A, Total Nitrogen and Total Phosphorus in Ulansuhai Lake. Advanced Materials Research. 955-959, 1393-1396. DOI:10.4028/www.scientific.net/amr.955-959.1393

Ho, J.C., Michalak, A.M. and Pahlevan, N. (2019) Widespread global increase in intense lake phytoplankton blooms since the 1980s. Nature. 574(7780), 667-670. DOI: 10.1038/s41586-019-1648-7

Huang, W., Zhang, J., Lepparanta, M., Li, Z., Cheng, B. and Lin, Z. (2019) Thermal structure and water-ice heat transfer in a shallow ice-covered thermokarst lake in central Qinghai-Tibet Plateau. Journal of Hydrology. 578, 124122. DOI: 10.1016/j.jhydrol.2019.124122

Kärkäs E. (2000) The Ice Season of Lake Pääjärvi in Southern Finland. Geophysica, 36(1–2), 85–94. DOI:

Karvonen, J., Shi, L., Cheng, B., Simila, M., Makynen, M. and Vihma, T. (2017) Bohai Sea Ice Parameter Estimation Based on Thermodynamic Ice Model and Earth Observation Data. Remote Sensing. 9(3), 234.DOI:10.3390/rs9030234

Kirillin, G., Lepparanta, M., Terzhevik, A., Granin, N., Bernhardt, J., Engelhardt, C., Efremova, T., Golosov, S., Palshin, N. and Sherstyankin, P.P. (2012) Physics of seasonally ice-covered lakes: a review. Aquatic Sciences. 74(4), 659-682. DOI: 10.1007/s00027-012-0279-y

Lei, A., Zhangli, H.U., Wang, J., Shi, Z. and Tam, F.N. (2005) Structure of the phytoplankton community and its relationship to water quality in Donghu Lake, Wuhan, China. Journal of Integrative Plant Biology. 47(1), 27-37.DOI:10.1111/j.1744-7909.2005.00020.x

Leppäranta, M., Tikkanen, M. and Virkanen, J. (2003) Observations of ice impurities in some Finnish lakes. Proceedings of the. Estonian Academy of Science. Chemistry 52(2), 59–75.

Lu, P., Cheng, B., Lepparanta, M. and Li, Z. (2018) Partitioning of solar radiation in Arctic sea ice during melt season. Oceanologia. 60(4), 464-477. DOI: 10.1016/j.oceano.2018.03.002

Merkouriadi, I., Cheng, B., Graham, R.M., Rosel, A. and Granskog, M.A. (2017) Critical Role of Snow on Sea Ice Growth in the Atlantic Sector of the Arctic Ocean. Geophysical Research Letters. 44(20). DOI:10.1002/2017GL075494

Michel, B. and Ramseier, R.O. (1971) Classification of river and lake ice. Canadian Geotechnical Journal. 8(1), 36-45. DOI:10.1139/t71-004

Moriasi, D.N., Arnold, J.G., Van Liew, M.W., Bingner, R.L., Harmel, R.D. and Veith, T.L. (2007) Model evaluation guidelines for systematic quantification of accuracy in watershed simulations. Trans. ASABE, 50, 885–900, DOI:10.13031/2013.23153.

Palmer, M.J., Chetelat, J., Richardson, M., Jamieson, H.E. and Galloway, J.M. (2019) Seasonal variation of arsenic and antimony in surface waters of small subarctic lakes impacted by legacy mining pollution near Yellowknife, NT, Canada. Science of The Total Environment. 684, 326-339. DOI: 10.1016/j.scitotenv.2019.05.258

Pennak and W., R. (1968) Field and Experimental Winter Limnology of Three Colorado Mountain Lakes. Ecology. 49(3), 505. DOI: 10.2307/1934117

Pieters, R. and Lawrence, G.A. (2009) Effect of salt exclusion from lake ice on seasonal circulation. Limnology & Oceanography. 54(2), 401-412.DOI:10.4319/lo.2009.54.2.0401

Powers, S.M., Labou, S.G., Baulch, H.M., Hunt, R.J., Lottig, N.R., Hampton, S.E. and Stanley, E.H. (2017) Ice duration drives winter nitrate accumulation in north temperate lakes. Limnology & Oceanography Letters. 2(5). DOI: 10.1002/lol2.10048

Prowse, T.D. (2001) River-Ice Ecology. I: Hydrologic, Geomorphic, and Water-Quality Aspects. Journal of Cold Regions Engineering. 15(1), 1-16. DOI: 10.1061/(ASCE)0887-381X(2001)15:1(1)

Shen, C., Liao, Q. and Bootsma, H.A. (2020) Modelling the influence of invasive mussels on phosphorus cycling in Lake Michigan. Ecological Modelling. 416, 108920.DOI:10.1016/j.ecolmodel.2019.108920

Shen, H.T. and Chiang, L.A. (1984) Simulation of Growth and Decay of River Ice Cover. Journal of Hydraulic Engineering. 110(7), 958-971. DOI:10.1061/(ASCE)0733-9429(1984)110:7(958)

Shen, H.T. and Yapa, P.D. (2011) A unified degree-day method for river ice cover thickness simulation. Canadian Journal of Civil Engineering. 12(1), 54-62. DOI:10.1139/l85-006

Sondergaard, M., Lauridsen, T.L., Johansson, L.S. and Jeppesen, E. (2017) Nitrogen or phosphorus limitation in lakes and its impact on phytoplankton biomass and submerged macrophyte cover. Hydrobiologia. 795(1), 35-48. DOI:10.1007/s10750-017-3110-x

Song, K., Wen, Z., Jacinthe, P., Zhao, Y. and Du, J. (2019) Dissolved carbon and CDOM in lake ice and underlying waters along a salinity gradient in shallow lakes of Northeast China. Journal of Hydrology. 571, 545-558. DOI: 10.1016/j.jhydrol.2019.02.012

Tido, S., Cheng, B., Yang, Y. and Laura, R. (2012) Snow and ice on Bear Lake (Alaska) – sensitivity experiments with two lake ice models, Tellus A: Dynamic Meteorology and Oceanography, 64:1, DOI: 10.3402/tellusa.v64i0.17339

Wang, X., Wei, J., Bai, N., Cha, H., Cao, C., Zheng, K. and Liu, Y. (2018) The phosphorus fractions and adsorption-desorption characteristics in the Ulansuhai Lake, China. Environmental Science and Pollution Research. 25(21), 20648-20661.DOI:10.1007/s11356-018-2233-6

Wei, Z. (2010) Satellite remote sensing data monitoring"Huang Tai"algae bloom in Lake Ulansuhai,Inner Mongolia. Journal of Lake Sciences. in Chinese.

Wu, T. and Qian, Z. (2003) The Relation between the Tibetan Winter Snow and the Asian Summer Monsoon and Rainfall: An Observational Investigation. Journal of Climate. 16(12), 2038-2051. DOI:10.1175/1520-0442(2003)016<2038:TRBTTW>2.0.CO;2

Yan, X., Xu, X., Ji, M., Zhang, Z., Wang, M., Wu, S., Wang, G., Zhang, C. and Liu, H. (2019) Cyanobacteria blooms: A neglected facilitator of CH4 production in eutrophic lakes. Science of The Total Environment. 651, 466-474. DOI: 10.1016/j.scitotenv.2018.09.197

Yang, B., Young, J., Brown, L. and Wells, M. (2017) High-Frequency Observations of Temperature and Dissolved Oxygen Reveal Under-Ice Convection in a Large Lake. Geophysical Research Letters. 44(24), 12,218-212,226. DOI:10.1002/2017GL075373

Yang, F., Changyou, L.I., Shi, X., Zhao, S. and Hao, Y. (2016a) Impact of seasonal ice structure characteristics on ice cover impurity distributions in Lake Ulansuhai. Journal of Lake Sciences. 28(2), 455-462. DOI:10.18307/2016.0226

Yang, F., Li, C., Lepparanta, M., Shi, X. and Zhang, C. (2016b) Notable increases in nutrient concentrations in a shallow lake during seasonal ice growth. Water Science & Technology. 74(12), 2773-2783. DOI:10.2166/wst.2016.433

Fang, Y., Feng W., Leppäranta, M., Yang, Y., Merkouriadi, I., Cen, R., Bai, Y., Li. C., and Liao H. (2020) Simulation and seasonal characteristic analysis of the intra-annual heat exchange process in a typical ice-covered lake. Sustainability. 12(18), 7832. DOI:/10.3390/su12187832

Yang, T., Hei, P., Song, J., Zhang, J., Zhu, Z., Zhang, Y., Yang, J., Liu, C., Jin, J. and Quan, J. (2019) Nitrogen variations during the ice-on season in the eutrophic lakes. Environmental Pollution. 247, 1089-1099. DOI:10.1016/j.envpol.2018.12.088

Yang, Y., Lepparanta, M., Cheng, B. and Li, Z. (2012) Numerical modelling of snow and ice thicknesses in Lake Vanajavesi, Finland. Tellus A. 64(1), 17202.DOI:10.3402/tellusa.v64i0.17202

Yao, Y., Huang, J., Luo, Y. and Zhao, Z. (2016) Improving the WRF model's (version 3.6.1) simulation over sea ice surface through coupling with a complex thermodynamic sea ice model (HIGHTSI). Geoscientific Model Development. 9(6), 2239-2254.DOI: 10.5194/gmd-9-2239-2016

Yu, Y., Cheng, B., Kourzeneva, E., Semmler, T. and Li, Z. (2013) Modelling experiments on air-snow-ice interactions over Kilpisjárvi, a lake in northern Finland. Boreal Environment Research. 18(5), 341-358. DOI: http://hdl.handle.net/10138/165155

Yuanyuan, F., Xing, L. and Xi, C. (2018) Research Progress of Eutrophication in Ulansuhai Sea. Environmental Protection Science.Chinese.

Zhang, Q., Yao, T., Huemmrich, K.F., Middleton, E.M., Lyapustin, A. and Wang, Y. (2020) Evaluating impacts of snow, surface water, soil and vegetation on empirical vegetation and snow indices for the Utqiaġvik tundra ecosystem in Alaska with the LVS3 model. Remote Sensing of Environment. 240, 111677. DOI:10.1016/j.rse.2020.111677

Zhang, Y., Li, C., Shen, H., Shi, X. and Qiao, L. (2013) Total nitrogen migration in Ulansuhai Lake during ice growth process. Advances in Water Science. 24(05),728-735.DOI: 10.14042/j.cnki.32.1309.2013.05.004

Zhang, Y., Li, C., Shi, X. and Li, C. (2012) The migration of total dissolved solids during natural freezing process in Ulansuhai Lake. Journal of Arid Land. 4(1), 85-94.DOI:10.3724/sp.J.1227.2012.00085

Zhang, Y., Tang, Y., Yu, A., Zhao, W. and Liu, Y. (2019) Research on the Migration of the Total Manganese during the Process of Water Icing. Water. 11(8), 1626. DOI: 10.3390/w11081626

Zhao, J., Cheng, B., Vihma, T., Yang, Q., Hui, F., Zhao, B., Hao, G., Shen, H. and Zhang, L. (2019) Observation and thermodynamic modeling of the influence of snow cover on landfast sea ice thickness in Prydz Bay, East Antarctica. Cold Regions Science and Technology. 168, 102869. DOI:10.1016/j.coldregions.2019.102869

Zhao, S., Shi, X., Li, C., Zhang, H. and Wu, Y. (2014) Seasonal variation of heavy metals in sediment of Lake Ulansuhai, China. Chemistry and Ecology. 30(1), 1-14.DOI:10.1080/02757540.2013.841894

Zubov, N.N. (1963) Arctic ice. U.S. Navy Electronics Laboratory, 510 pp. Google Scholar

Figure captions

Figure 1. The water environment monitoring points of Ulansuhai Lake

Figure 2. Water and solution balance in a water column unit

Figure 3. The air temperature and ice cover growth simulation during the winter of 2013 to 2014 (The freezing date was November 10, 2013. The date of the temperature began to rise was February 22, 2014.)

Figure 4. The measured data and the simulated value of ice thickness from 2007 to 2014 (The numbers on top of the bars were sample quantity for each year.)

Figure 5. Ice cover growth modeled by HIGHTSI during the winter of 2010 to 2014 (The error bar indicated the range of ice thickness measurements.)

Figure 6. TN and TP variation in water under the ice cover from 2008 to 2014(The blue bars were observations. The purple bars indicated the mean of observed.)

Figure 7. The simulation results of TN variation in lake water under different distribution coefficients: (a) based on empirical degree-day model and (b) based on the HIGHTSI

Figure 8. The simulation results of TP variation in lake water under different distribution coefficients: (a) based on empirical degree-day model and (b) based on the HIGHTSI

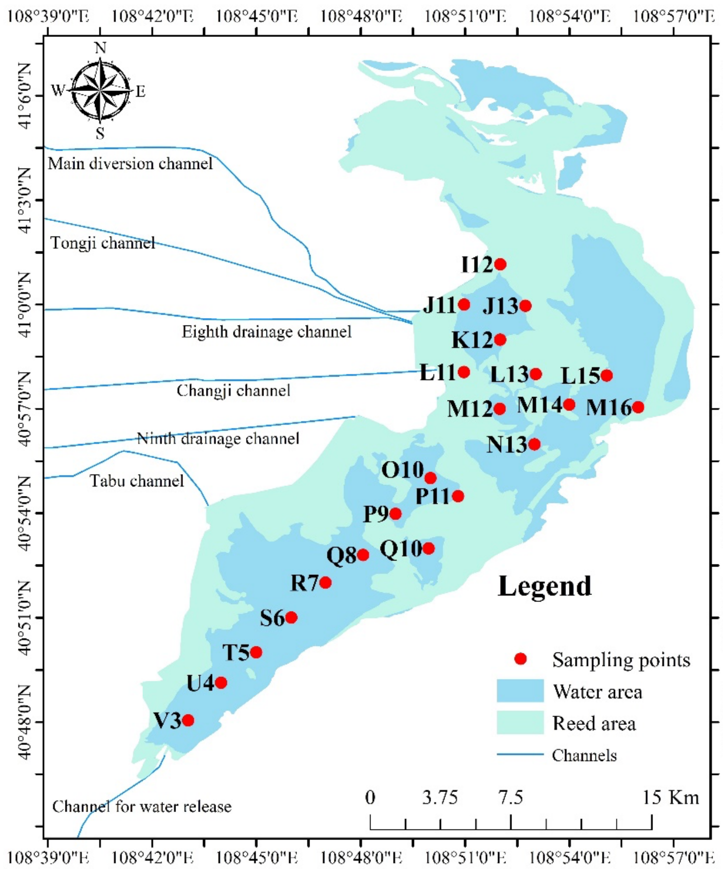

Figure 1. The water environment monitoring points of Ulansuhai Lake

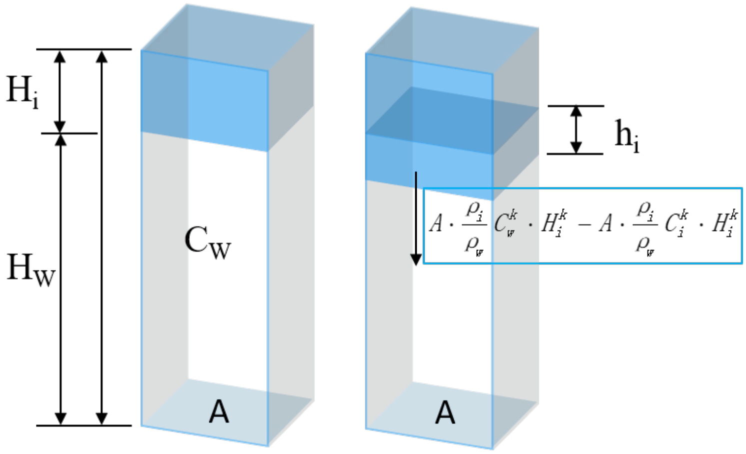

Figure 2. Water and solution balance in a water column unit

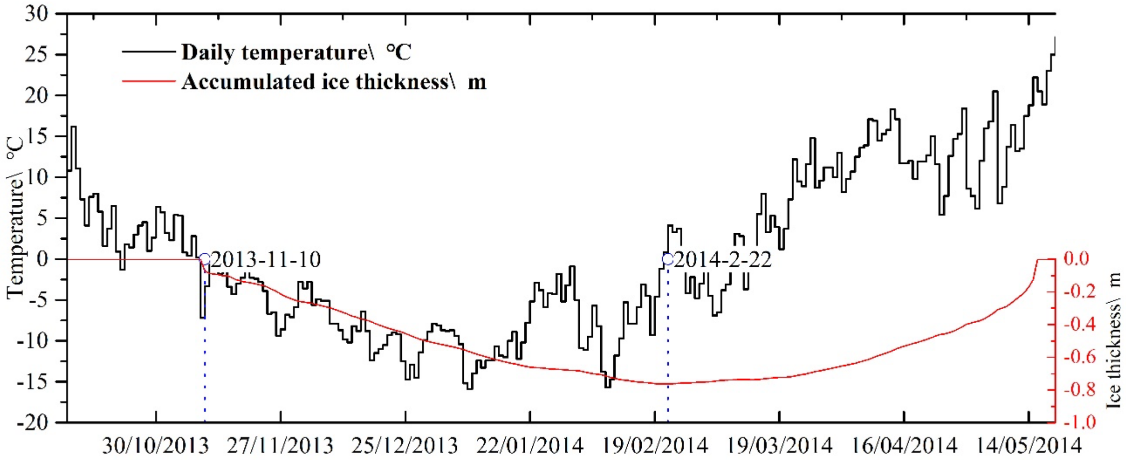

Figure 3. The air temperature and ice cover growth simulation during the winter of 2013 to 2014 (The freezing date was November 10, 2013. The date of the temperature began to rise was February 22, 2014.)

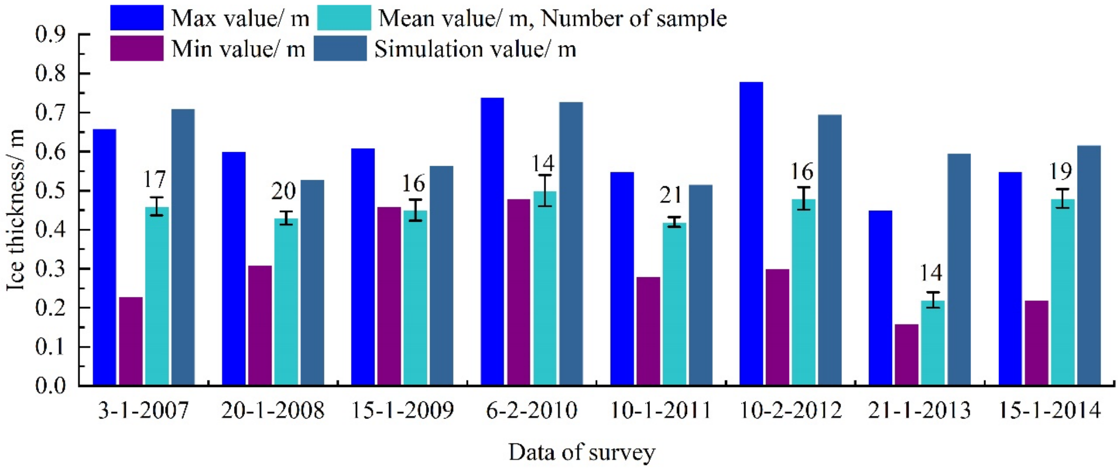

Figure 4. The measured data and the simulated value of ice thickness from 2007 to 2014 (The numbers on top of the bars were sample quantity for each year.)

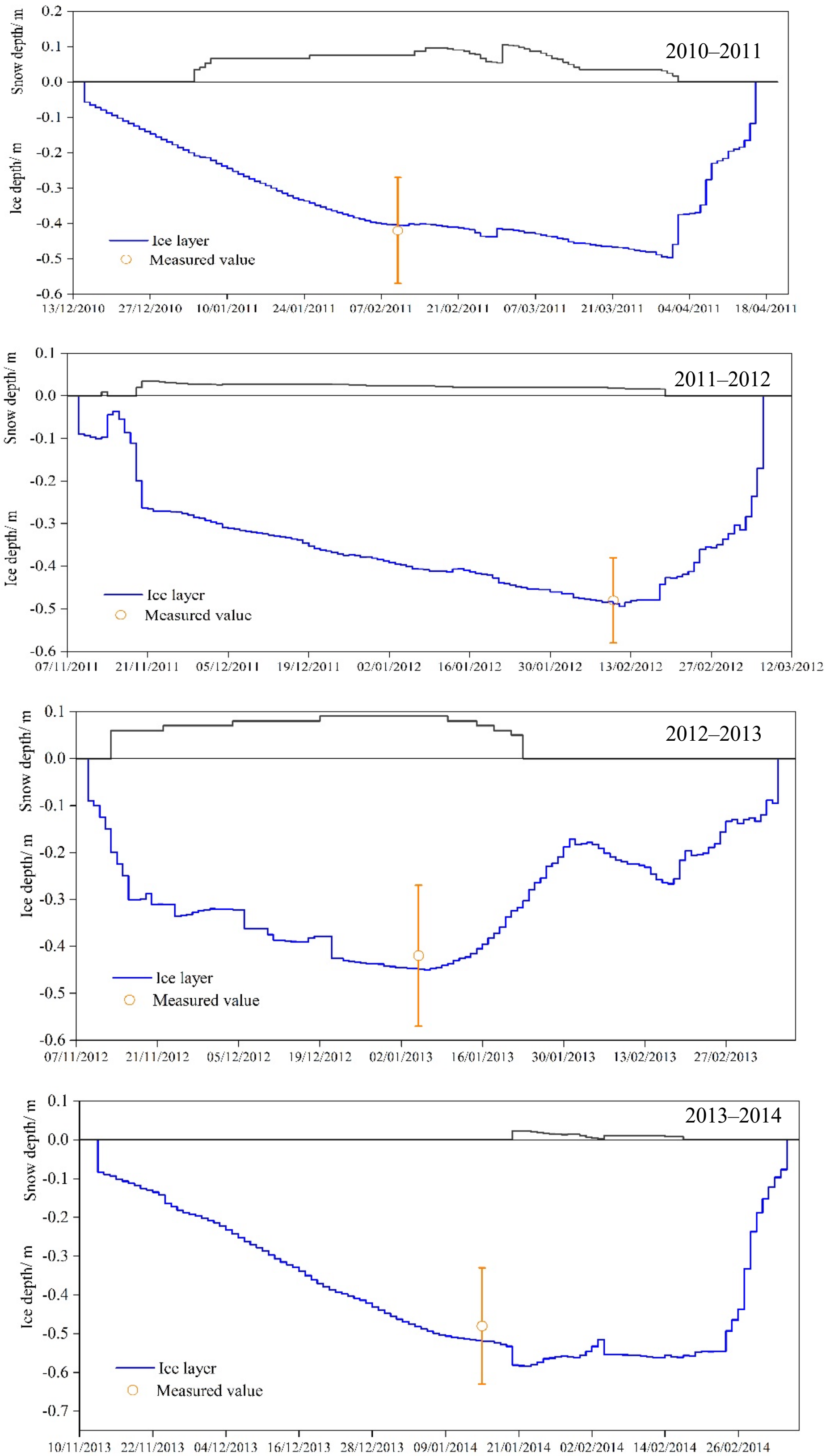

Figure 5. Ice cover growth modelled by HIGHTSI during the winter of 2010 to 2014 (The error bar indicated the range of ice thickness measurements.)

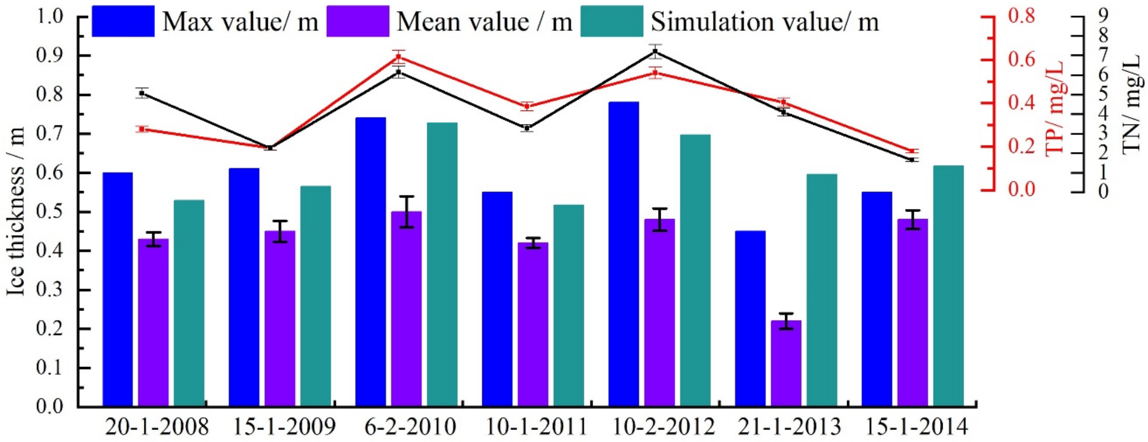

Figure 6. TN and TP variations in water under the ice cover from 2008 to 2014 (The blue bars were observations. The purple bars indicated the mean of observed.)

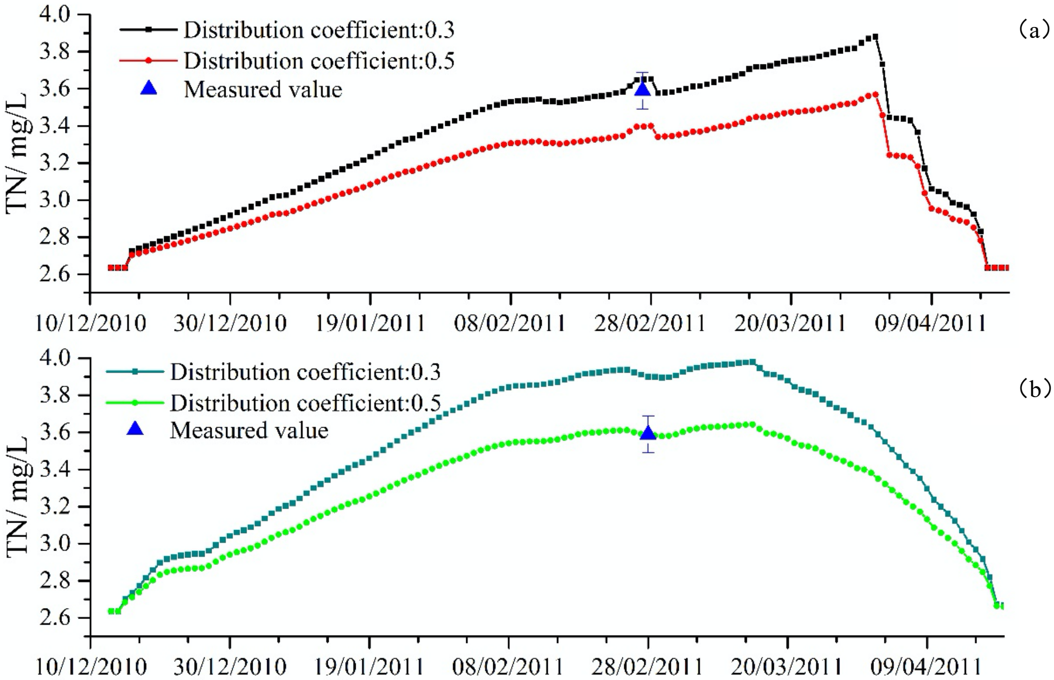

Figure 7. The simulation results of TN variation in lake water under different segregation coefficients: (a) based on empirical degree-day model and (b) based on the HIGHTSI

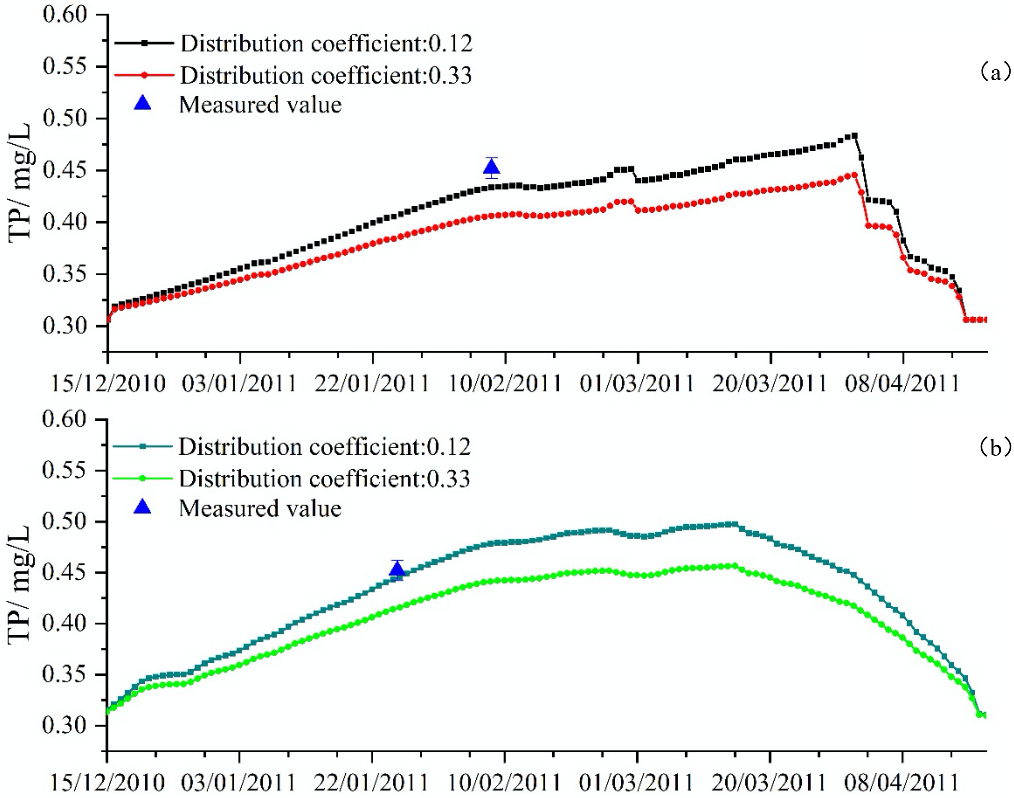

Figure 8. The simulation results of TP variation in lake water under different segregation coefficients: (a) based on empirical degree-day model and (b) based on the HIGHTSI

Table 1. Typical values of the parameter A_0 (Michel and Ramseier, 1971)

Ice cover conditions	Snowless windy lake	Snowless average lake	Snowless average river	Screened rapids
$A_0 (cm \cdot C^{-1/2} \cdot day^{-1/}$	2.7	1.7–2.4	1.3–1.7	0.7–1.4

Table 2. Input parameters and output values of model of HIGHTSI

Parametertype	**Parameter**
Input meteorological data series	Wind speed (m/s)
	Temperature (°C)
	Relative humidity (%)
	Cloud cover (1–8)
	Precipitation (mm)
Input model parameters	Total calculation steps
	Initial date
	Initial time
	Snow cover albedo
	Ice cover albedo
	Latitude
	Meteorological observation altitude
	Thermal conductivity of snow
	Thermal conductivity of ice
	Salinity
Output calculated value	Calculated ice thickness
	Calculated snow thickness
	Solar radiation flux
	Latent heat flux
	Sensible heat flux
	Snow temperature
	Ice temperature

Table 3. Basic parameters comparison and selection

References	Sea ice (Kärkäs E, 2000)	Vanajavesi Lake	Ulansuhai Lake
Ice density (kg/m^3)	910	1000	1000
Ice thermal conductivity (W/(m·k))	2.03	2.1	2.1
Ice salinity (‰)	Relationship between salinity and ice growth-rate	0	0.1
Freezing point ℃	-1.9	-0.5	-0.5
Initial snow thickness (cm)		0.5	0.01 m
Initial ice thickness(cm)		2	0.1 m
Timestep		1 h	1 h
Initial model-run date		1/1/2009	Day 3 of a consecutive 3-day period with daily mean temperature below 0℃
Calculation period		1/2009-4/2009	12/2010-4/2011; 11/2011-3/2012;11/2012-3/2013;11/2013-3/2014
Ice-melt day		29/4/2009	2011.4.14;2011.3.10;2011.3.7;2011.3.9
Calculation step		2856	2904;2952;2808;2736

Table 4. Ulansuhai ice thickness simulation with degree-day empirical model from 2006 to 2014

Freeze date	Temperature rise date	Continuous negative temperature duration (d)	Cumulative negative temperature (°C·d)	Predicted ice thickness m	Temperature rising stage
17/11/2006	11/3/2007	93	-764.5	0.747	18/2/2007–3/3/2007
15/11/2007	3/3/2008	110	-860.8	0.792	
16/11/2008	4/3/2009	100	-610.5	0.667	2/2/2009–14/2/2009
1/11/2009	19/2/2010	105	-849.6	0.787	3/11/2009–10/11/2009
15/12/2010	15/3/2011	100	-768.3	0.748	
22/11/2011	12/3/2012	111	-782.1	0.755	
10/11/2012	23/2/2013	105	-751.9	0.740	
10/11/2013	21/2/2014	104	-799.3	0.763	

Supplementary information

SI 1 Empirical model of smoothed lake ice cover

The ice cover in Ulansuhai Lake is formed through thermal growth. The ice thickness can be calculated using a degree-day growth model (Stefan, 1891). If only the primary factors affecting the growth rate of ice cover, such as ice cover thickness and surface temperature, are considered, then the growth rate of ice cover is given by:

$$\frac{dH}{dt} = -\frac{\lambda_i}{H\rho_i L}\left(T_0 - T_f\right) \quad (1)$$

where ρ_i is the ice density (916 kg/m^3), L is the specific heat of ice (3.34 x 10^5 J/kg), λ_i is the thermal conductivity of ice (2.24 W/m ºC), T_0 is the temperature of the upper ice-surface, and T_f is the temperature of the lower ice-surface.

Based on typical approximation assumptions (Stefan, 1891), the upper surface of the ice cover is assumed to be equal to the atmospheric temperature, T_a. Then the integral of ice growth rate over time is:

$$\frac{1}{2}H^2 = \frac{\lambda_i}{\rho_i L}\int_0^{t_e}\left(T_f - T_a\right)dt \quad (2)$$

Also, a parameter θ, defined below, is often introduced.

$$\theta = \int_0^{t_e}\left(T_f - T_a\right)dt \quad (3)$$

Based on results of previous theoretical studies (Leppäranta, 1993), if the time interval (Δt) input into the degree-day growth model of sea ice is one day, and θ is the cumulative negative temperature sum (ºC d) during ice season, then the ice cover thickness *H* is related to the cumulative number of degree-day θ below the freezing temperature since the formation of the initial ice cover. The freezing-degree-days can be obtained from meteorological data, and then the ice thickness is obtained from

$$\frac{1}{2}H^2 = \frac{\lambda_i}{\rho_i L}\theta \quad (4)$$

The equation can be simplified to:

$$H = A_0\theta^{1/2} \quad (5)$$

where A_0 is an empirical constant. Some studies have provided the values of A_0 under different ice conditions (Michel and Ramseier, 1971), as shown in Table 1. This equation is not suitable for simulating ice cover during the ablation period. When using the empirical equation, we assume that A_0 = 2.7 cm $C^{-1/2}$ $day^{-1/2}$. Then, the empirical formula becomes:

$$H = 0.027\theta^{1/2} \quad (6)$$

SI 2 HIGHTSI model

The HIGHTSI model is a one-dimensional thermodynamic numerical model of atmosphere-ice-seawater/freshwater (Cheng and Launiainen, 2003). The model describes the freezing process of natural water bodies through a parameterization scheme and numerical analysis based on the Fortran language. The main input parameters and output values are listed in Table 2. with parameter modification, the model can be used to predict the growth of freshwater ice and snow cover in lakes and reservoirs (Yang et al., 2012).

The calculation process consists of the following four main processes, as shown in Fig. S1 (Cheng and Launiainen, 2003): (1) heat exchange between the atmosphere and ice/water interface (I. ABL), (2) internal heat conduction and phase transition of ice/snow (II), (3) thermal ice growth process (III Ice), and (4) and heat conduction at the ice–water interface (IV Water layer).

The HIGHTSI model is a numerical simulation model of ice thickness based on the heat conduction. By identifying the physical characteristics of the research object and optimizing the model parameters, the thickness of ice and snow cover can be simulated using meteorological data series as the input. The forcing term is the input meteorological data, the heat flux from the water body, and the given initial ice and snow cover thickness.

SI 3 Nutrient distribution coefficient

SI 3.1 Simulation experiment control conditions

Under typical conditions, in fall water cools down at the lake surface, because it is in contact with the atmosphere, and then the ice grows downward from the surface. To simulate this process by physical experiments, thermal insulation should be applied to the experimental equipment. Figure S2 shows the constant temperature freezer box used as the indoor freezing simulation device. The interior of the box is lined with a 5 cm thick foam board. Custom-made, open-top plexiglass sampling cylinders (5 cm wall thickness, 10 cm diameter, and 50 cm height) were wrapped with thermal insulation cotton and then wrapped again with thermal insulation bubble wrap. Next, the insulated cylinders were filled with water samples and placed inside the freezer box. The space between the cylinders was filled with small Styrofoam pellets to ensure that a minimal amount of heat was dissipated from the cylinders. The top of the cylinders remained open to ensure that the freezing process commenced from the surface and advanced toward the bottom.

Based on the samples collected in the winter 2010–2011, the ice thickness of Ulansuhai Lake reached 21–62 % of the water depth, and the mean volume ratio of ice to water was approximately 1:2 (Yang et al. 2012). During the simulation experiment, the initial water level in the sampling cylinders was set at 45 cm. After the ice thickness reached 15 cm, the ice layer and the water below were extracted from the cylinder. The volume ratio of the ice layer to the water was 1:2. Unfrozen water was run out using a tap on the side of the cylinder to prevent water from mixing with the ice during the pouring process. During the experiment, the expansion of ice caused some damage to the sampling cylinders, which were checked regularly and replaced if necessary.

SI 3.2 Determination of the nutrient determination coefficient

Table S1 shows the segregation coefficients of nutrients in ice and the underlying water under different initial conditions. It is evident that as the initial concentration decreased, the segregation coefficient increased. The segregation coefficients of TP and TN were 0.33–0.12 and 0.50–0.30, respectively. In practical applications, an appropriate segregation coefficient can be selected based on the initial concentration of lake water nutrients before the formation of ice cover to estimate of the nutrient content of the water under the ice.

Table S2 shows the segregation coefficients of nutrients, ice, and the underlying water at different temperatures. As the temperature decreases, the distribution ratio of nutrients increases markedly, showing that the cooling rate in early winter has a considerable impact on the amount of nutrients in the ice cover.

References

Leppäranta M. A review of analytical models of sea-ice growth. Atmosphere-Ocean, 1993, 31(1): 123-138.

Michel B, Ramseier R O. Classification of river and lake ice. Canadian Geotechnical Journal, 1971, 8(1): 36-45.

Yang Y, Leppäranta M, Cheng B, et al. Numerical modelling of snow and ice thicknesses in Lake Vanajavesi, Finland. Tellus, 2012, 64(3):53-66.

Cheng B, Launianen J, Vihma T. Modelling of Superimposed Ice Formation and SubSurface Melting in the Baltic Sea. Geophysica, 2003.

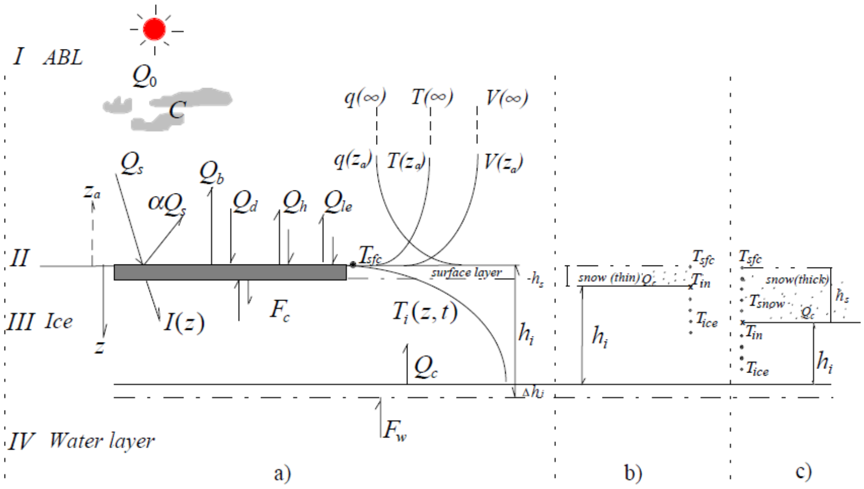

SI. Fig. 1. Schematic diagram of heat exchange mechanism in ice-covered lake（a. atmospheric boundary layer; b. thin snow; c. thick snow）

702 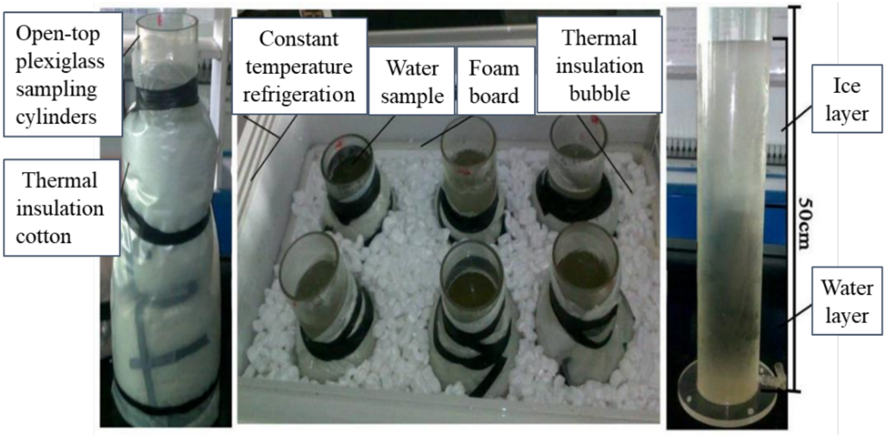

703 SI. Fig. 2. Experimental setup of freezing simulation

SI. Table 1 Segregation coefficients of nutrients between ice and water in different initial concentrations

Solute	Sample point	Initial concentration C_w^0	Mean concentration in ice $\overline{C_i}$	Under-ice water concentration C_w	segregation coefficient $k = \overline{C_i}$	Under-ice water concentration $n = C_w$
TP	I12	0.46	0.30±0.001	0.92±0.001	0.33	2.00
	M12	0.13	0.15±0.001	0.84±0.001	0.18	6.46
	Q8	0.08	0.09±0.003	0.73±0.001	0.12	9.13
TN	I12	2.96	2.63±0.001	5.22±0.001	0.50	1.76
	M12	2.17	1.83±0.001	4.74±0.001	0.39	2.18
	Q8	1.38	1.05±0.002	3.53±0.001	0.30	2.56

SI. Table 2 Nutrient distribution coefficient between ice and under-water for different temperature after freezing

Solute	Initial concentration C_w^0	Mean concentration in ice $\overline{C_i}$ (Error limit a ≤ ± 5%)			Under-ice water concentration C_w (Error limit a ≤ ± 5%)			Distribution coefficient $k = \overline{C_i} / C_w$		
		-25℃	-20℃	-15℃	-25℃	-20℃	-15℃	-25℃	-20℃	-15℃
TP	0.32	0.18	0.15	0.12	0.38	0.40	0.43	0.49	0.38	0.28
TN	2.70	1.87	1.78	1.70	3.18	3.21	3.67	0.59	0.55	0.46